NUMERICAL STUDY OF NATURAL CONVECTION IN AN INCLINED CAVITY WITH PARTIALLY ACTIVE SIDE WALLS FILLED WITH CU-WATER NANOFLUID

G.A. Sheikhzadeh*

Department of Mechanical Engineering, University of Kashan, Kashan, Iran
Sheikhz@kashanu.ac.ir

A. Arefmanesh

Department of Mechanical Engineering, University of Kashan, Kashan, Iran
arefmanesh@kashanu.ac.ir

M.H. Kheirkhah

Department of Mechanical Engineering, University of Kashan, Kashan, Iran
kheirkhahmh@yahoo.com

R. Abdollahi
Department of Mechanical Engineering, University of Kashan, Kashan, Iran
Rat_2003@yahoo.com

*corresponding author

(Received: May 24, 2010 – Accepted in Revised Form: September 15, 2011)

doi: *10.5829/idosi.ije.2011.24.03b.08*

Abstract The buoyancy-driven fluid flow and heat transfer in a square cavity with partially active side walls filled with Cu-water nanofluid is investigated numerically. The active parts of the left and the right side-walls of the cavity are maintained at temperatures T_h and T_c, respectively, with $T_h>T_c$. The enclosure's top and bottom walls, as well as, the inactive parts of its side walls are kept insulated. The governing equations are discretized using the finite volume method and the hybrid scheme. Using the developed code, a parametric study is undertaken and the effects of the Rayleigh number, the locations of the active parts of the side walls, the volume fraction of nanoparticles, and inclination angle of cavity on the fluid flow and heat transfer inside the cavity are investigated. It is observed from the results that the average Nusselt number increases with increasing both the Rayleigh number and the volume fraction of the nanoparticles. Moreover, the maximum average Nusselt number occurs for the middle-middle location of the thermally active parts.

Keywords Nanofluid**,** Natural convection**,** Partially active walls**,** Cavity

چکیده جریان سیال و انتقال حرارت جابجایی آزاد در یک محفظه مربعی شکل با دیواره‌های جانبی به طور جزئی فعال که حاوی نانوسیال آب- مس می‌باشد، به طور عددی بررسی می‌شود. قسمت‌های فعال دیواره‌های جانبی چپ و راست محفظه به ترتیب در دماهای T_h و T_c ($T_h>T_c$) قرار دارند. دیواره‌های بالا و پایین محفظه و قسمت‌های غیر فعال دیواره‌های جانبی عایق می‌باشند. معادلات حاکم با استفاده از روش حجم محدود و طرح پیوندی منفصل می‌شوند. با استفاده از کد کامپیوتری توسعه داده شده یک مطالعه پارامتری انجام می‌شود و اثرات عدد رایلی، محل قسمت فعال دیواره های جانبی، کسر حجمی نانوذرات بر جریان سیال و انتقال حرارت درون محفظه و زاویه انحراف محفظه مورد بررسی قرار می‌گیرد. نتایج نشان می‌دهد که عدد ناسلت متوسط با افزایش عدد رایلی و کسر حجمی نانوذرات افزایش می‌یابد. علاوه بر این، بیشترین مقدار عدد ناسلت میانگین برای حالت وسط- وسط قسمت‌های فعال گرمایی رخ می‌دهد.

Nomenclature

c_p	specific heat (kJ kg^{-1} K^{-1})
g	gravitational acceleration (m s^{-2})
h	heat transfer coefficient (W m^{-2} K^{-1})
L	enclosure length (m)
k	thermal conductivity (W m^{-1} K^{-1})
Nu	Nusselt number
Nu_{avg}	average Nusselt number
p	pressure (Nm^{-2})
P	dimensionless pressure
Pr	Prandtl number
Ra	Rayleigh number
T	temperature (K)
u, v	velocity components (m s^{-1})
U, V	Dimensionless velocity components

Greek symbols

α	thermal diffusivity (m^2 s^{-1})
β	thermal expansion coefficient (K^{-1})
φ	nanoparticle volume fraction
ν	kinematic viscosity (m^2 s^{-1})
θ	dimensionless temperature
Ψ	stream function (m^2 s^{-1})
ρ	density (kg m^{-3})
μ	dynamic viscosity (N s m^{-2})
γ	angle of inclination of the cavity

Subscripts

nf	nanofluid
f	fluid
h	Hot
c	cold
s	Solid

1. INTRODUCTION

Natural convection heat transfer is an important phenomenon in engineering and industry with widespread applications in diverse fields, such as, geophysics, solar energy, electronic cooling, and nuclear energy to mention a few. A major limitation against increasing the heat transfer in such engineering systems is the inherently low thermal conductivity of the commonly used fluids, such as, air, water, and oil. Nanofluids were introduced in order to circumvent the above limitation [1]. A nanofluid is a dilute suspension of solid nanoparticles with the average size below 100nm in a base fluid, such as, water, oil, and ethylene glycol. Nanofluids exhibit thermal properties superior to those of the base fluids of the conventional particle-fluid suspensions [2].

A number of studies have been devoted to investigate the properties of the nanofluids. Xuan and Li [3] used the hot-wire apparatus to measure the thermal conductivity of nanofluids. They investigated the effect of the volume fraction and the dimensions, shapes, and thermo-physical properties of the nanoparticles on the thermal conductivity of the nanofluids.

In another experimental work, Xie et al. [4] investigated the dependence of the thermal conductivity of the nanoparticle-fluid mixture on the base fluid. Their results showed that nanoparticle-fluid mixtures, containing only a small amount of the nanosized Al_2O_3 particles, had substantially higher thermal conductivities compared to that of the pure fluid. Heyhat and Kowsary [5] studied the wall shear stress and heat transfer coefficient of γAl_2O_3-water nanofluids under laminar forced convection through a circular pipe numerically. Their results showed that adding γAl_2O_3 nanoparticles to pure water effectively enhanced the convective heat transfer and the wall shear stresses.

The forced convection, as well as, the buoyancy-driven fluid flow and heat transfer in enclosures have been studied by several investigations. Shokouhmand and Sayehvand [6] used the SIMPLER algorithm to simulate the fluid flow and heat transfer in a lid-driven square cavity for the Reynolds numbers between 1 and 10^4. Their results showed that an inviscid core region was developed in the cavity at sufficiently high values of the Reynolds number. Moreover, secondary eddies were always present in the bottom corners of the cavity.

Khanafer et al. [7] considered the heat transfer enhancement in a two-dimensional cavity filled with nanofluids for the Grashof numbers of 10^3, 10^4 and 10^5 using the finite volume method. They concluded that the existence of the nanoparticles resulted in an increase in the rate of heat transfer for all the considered Grashof numbers. Using the finite volume method, Maiga et al. [8] studied the problem of laminar forced convection flow of nanofluids in a uniformly heated tube, as well as, a system of parallel, coaxial and heated disks. Their results showed that the inclusion of Al_2O_3 nanoparticles in water and ethylene-glycol

resulted in a considerable augmentation of the heat transfer coefficient in the considered geometrical configurations. Jou and Tzeng [9] conducted a numerical study on the natural convection heat transfer in rectangular enclosures filled with nanofluid using the finite difference method and the stream function-vorticity formulation. They investigated the effects of the Rayleigh number, the aspect ratio of the enclosure, and the volume fraction of the nanoparticles on the heat transfer inside the enclosures. Their results showed that the average heat transfer coefficient increased with increasing the volume fraction of the nanoparticles. More recently, Polidori et al. [10] used the integral formulation approach to investigate the natural convection heat transfer of Alumina-water nanofluid in a laminar, external and boundary layer flow. They examined different viscosity models and concluded that, in addition to the nanofluid thermal conductivity, its viscosity also played a significant role in the heat transfer enhancement.

Enclosures with partially active side walls have special importance in the convection heat transfer field because of their wide applications in industry, such as, cooling of electronic heater. However, limited numerical studies have been performed on these enclosures. The buoyancy-driven heat transfer in square cavities filled with air with partially active vertical walls was studied numerically by Valencia and Frederick [11]. They considered different relative positions of the active parts of the walls for the Rayleigh numbers of 10^3-10^7. Their results showed that the maximum heat transfer occurred for the heat source positioned at the middle of the hot wall. Deng et al. [12] used the finite volume method to study the laminar natural convection in a rectangular enclosure with discrete heat sources on its side walls. They concluded that an isothermal heat source had a stronger effect on the fluid flow and heat transfer inside the cavity compared to a constant flux one. The natural convection heat transfer in a square cavity filled with air with partially active side walls was studied by Nithyadevi et al. [13] using the finite volume method. They investigated the effects of the aspect ratio of the cavity and different relative positions of the active zones on the heat transfer inside the cavity. Their results showed that the heat transfer rate was high for the bottom-top thermally active location while it was low for the top-bottom thermally active location. The magneto-convection in a cavity with partially active walls was investigated numerically by Sheikzadeh et al. [14]. They considered the effects of different parameters such as the Rayleigh number, Hartmann number, aspect ratio, and inclination angle on the heat transfer rate. Their results showed that the average Nusselt number decreased with increasing the Hartmann number, and increased with increasing the Rayleigh number.

Very recently, Oztop and Abu-Nada [15] employed the finite volume method to study the natural convection in rectangular enclosures with heaters on their left vertical walls filled with nanofluids. They investigated the effect of the Rayleigh number, heater height, location of the heater, aspect ratio of the cavity, and the volume fraction of the nanoparticles on the heat transfer inside the enclosures. They found that the mean Nusselt number increased with the volume fraction of the nanoparticles. Moreover, the heater location affected the flow and temperature fields inside the cavities.

There are a number of studies on the effect of the inclination angle on the fluid flow and heat transfer in a cavity containing pure fluid. Polentini et al. [16] investigated experimentally the effect of aspect ratio and the tilting angle of the cavity having a 3×3 array of flash-mounted discrete heat sources on one wall which are cooled by an apposing wall. Their results showed that by increasing the inclination angle, the heat transfer enhanced in heaters. Kenjeres et al. [17] studied the effect of the inclination angle on the natural convection in a cubical cavity filled air. The natural convection in tilted square cavities with differentially heated opposite walls filled air was studied by Cianfrini et al. [18]. They investigated the influence of changing of the inclination angle from 0 to 360°, and the Rayleigh number from 10^4 to 10^6 on the heat transfer rate and fluid flow in the cavity. Baïri [19] investigated numerically and experimentally the natural convection in 2D, titled, square enclosures filled air. He presented the Nusselt- Rayleigh correlations for different inclination angle of the cavity. The free

convection in a cubic cavity consist of a cool vertical wall and another wall with three heat bands and two adiabatic bands filled air was studied by Baïri et al. [20]. They considered the effect of the tilt angle of cavity between 0 to 360° on the heat transfer and fluid flow using experimental and numerical approaches.

Quite recently Corcione and Habib [21] studied numerically the natural convection in a partially active wall cavity using the SIMPLE-C algorithm. They considered the effect of the Rayleigh number, the Prandtl number and the inclination angle of cavity (from -75° to 75°) on the heat transfer. Their results showed that for negative inclination angles, the heat transfer increased with increasing the angle.

The main objective of the current study is to investigate the effect of the location of partially active side walls and the inclination angle on the heat transfer characteristics of a square cavity containing a nanofluid. In the present study, the natural convection in a square cavity with partially active side walls filled with Cu-water nanofluid is studied numerically using the finite volume method. A parametric study is performed and the effects of pertinent parameters, such as, the locations of the heat source and the heat sink on the side-walls, the Rayleigh number, and the volume fractions of the nanofluid on the fluid flow and heat transfer inside the enclosure are investigated.

2. PROBLEM FORMULATION

A schematic diagram of the inclined square cavity with the length equal to L is shown in Figure 1. An isothermal heat source with the temperature T_h, and a heat sink with the constant temperature of T_c ($T_h>T_c$) are placed along the left and the right side-walls of the cavity, respectively. The length of the heat source which is the same as that of the heat sink is equal to $L/2$ (Figure 1). The positions of the source and the sink along the side walls are symmetric with respect to the centerlines of the cavity for the case shown in this Figure. This configuration of the source and the sink is called middle-middle for brevity. Other configurations are generated by changing the relative positions of the source and the sink on the walls. The top and the bottom walls of the cavity, as well as, the inactive portions of the side walls are kept insulated. The cavity is filled with the Cu-water nanofluid which is assumed to be Newtonian. The nanoparticles are assumed to be uniform in shape and size. Moreover, the base fluid and the nanoparticles are assumed to be in thermal equilibrium. Other assumptions are that the flow is incompressible and there is not any slip between the water and the nanoparticles. The thermo-physical properties of the nanofluid are considered to be constant with the exception of its density which varies according to the Boussinesq approximation.

The steady-state continuity, momentum, and energy equations for the laminar, incompressible and buoyancy-driven fluid flow and heat transfer of the nanofluid inside the cavity using the Boussinesq approximation for the buoyancy term are given by:

$$\frac{\partial u}{\partial x}+\frac{\partial v}{\partial y}=0 \tag{1}$$

$$\rho_{nf}\left(u\frac{\partial u}{\partial x}+v\frac{\partial u}{\partial y}\right)=-\frac{\partial p}{\partial x}+\mu_{nf}\left(\frac{\partial^2 u}{\partial x^2}+\frac{\partial^2 u}{\partial y^2}\right)+g\sin\gamma(\rho\beta)_{nf}(T-T_c) \tag{2}$$

$$\rho_{nf}\left(u\frac{\partial v}{\partial x}+v\frac{\partial v}{\partial y}\right)=-\frac{\partial p}{\partial y}+\mu_{nf}\left(\frac{\partial^2 v}{\partial x^2}+\frac{\partial^2 v}{\partial y^2}\right)+g\cos\gamma(\rho\beta)_{nf}(T-T_c) \tag{3}$$

$$u\frac{\partial T}{\partial x}+v\frac{\partial T}{\partial y}=\alpha_{nf}\left(\frac{\partial^2 T}{\partial x^2}+\frac{\partial^2 T}{\partial y^2}\right) \tag{4}$$

Where u and v are the velocity components in the x and y-directions, respectively, p is the pressure, T is the temperature, φ is the volume fraction of the nanoparticles, and β is the thermal expansion coefficient. The thermo-physical properties of the nanofluid are obtained from the following relations [7, 22]:

$$\rho_{nf}=(1-\varphi)\rho_f+\varphi\rho_s \tag{5}$$

$$(\rho c_p)_{nf}=(1-\varphi)(\rho c_p)_f+\varphi(\rho c_p)_s \tag{6}$$

$$(\rho\beta)_{nf}=(1-\varphi)(\rho\beta)_f+\varphi(\rho\beta)_s \tag{7}$$

$$\frac{k_{nf}}{k_f}=\frac{k_s+2k_f-2\varphi(k_f-k_s)}{k_s+2k_f+\varphi(k_f-k_s)} \tag{8}$$

$$\alpha_{nf}=\frac{k_{nf}}{(\rho c_p)_{nf}} \tag{9}$$

$$\mu_{nf}=\frac{\mu_f}{(1-\varphi)^{2.5}} \tag{10}$$

The thermo-physical properties of the base fluid and the nanoparticles (at 300K) are presented in Table 1.

TABLE 1. Thermo physical properties of the base fluid and the nanoparticles

Properties	Base fluid (water)	Nanoparticles (Cu)
μ(Nsm^{-2})	8.55×10^{-4}	-
c_p(Jkg^{-1}K^{-1})	4179	385
ρ (kgm^{-3})	997.1	8933
k (Wm^{-1}K^{-1})	0.613	401
β (K^{-1})	2.761×10^{-4}	1.67×10^{-5}
α (m^{2}s^{-1})	1.47×10^{7}	1.17×10^{-4}

Using the dimensionless variables

$$X=\frac{x}{L}\quad,\quad Y=\frac{y}{L}\quad,\quad U=\frac{uL}{\alpha_{nf}}\quad,\quad V=\frac{vL}{\alpha_{nf}}$$
$$P=\frac{pL^2}{\rho_{nf}\alpha_{nf}^2}\quad,\quad \theta=\frac{T-T_c}{T_h-T_c} \tag{11}$$

the governing equations are written in the following dimensionless form:

$$\frac{\partial U}{\partial X}+\frac{\partial V}{\partial Y}=0, \tag{12}$$

$$U\frac{\partial U}{\partial X}+V\frac{\partial U}{\partial Y}=-\frac{\partial P}{\partial X}+\Pr\left(\frac{\partial^2 U}{\partial X^2}+\frac{\partial^2 U}{\partial Y^2}\right)+Ra\Pr\theta\sin\gamma, \tag{13}$$

$$U\frac{\partial V}{\partial X}+V\frac{\partial V}{\partial Y}=-\frac{\partial P}{\partial Y}+\Pr\left(\frac{\partial^2 V}{\partial X^2}+\frac{\partial^2 V}{\partial Y^2}\right)+Ra\Pr\theta\cos\gamma, \tag{14}$$

$$U\frac{\partial \theta}{\partial X}+V\frac{\partial \theta}{\partial Y}=\left(\frac{\partial^2 \theta}{\partial X^2}+\frac{\partial^2 \theta}{\partial Y^2}\right) \tag{15}$$

In the above equations, the Prandtl number (Pr) and the Rayleigh number (Ra) are defined as:

$$Ra=\frac{g(\rho\beta)_{nf}(T_h-T_c)L^3}{\mu_{nf}\alpha_{nf}}\quad,\quad Pr=\frac{\nu_{nf}}{\alpha_{nf}}. \tag{16}$$

The dimensionless boundary conditions are given by:

$$\begin{aligned} &U \,\&\, V=0, && \text{on the walls}\\ &\theta=0, && \text{on the sink}\\ &\theta=1, && \text{on the source}\\ &\partial\theta/\partial n=0 && \text{on the adiabatic wall} \end{aligned} \tag{17}$$

where $\partial/\partial n$ denotes the derivative with respect to the normal direction. Having obtained the temperature distribution, the average Nusselt number is calculated using the following relation:

$$Nu_{avg}=2\frac{k_{nf}}{k_f}\int_{Y_1}^{Y_2}\left.\frac{\partial\theta}{\partial X}\right|_{X=0}dY \tag{18}$$

where the dimensionless coordinates Y_1 and Y_2 are defined in Figure 1.

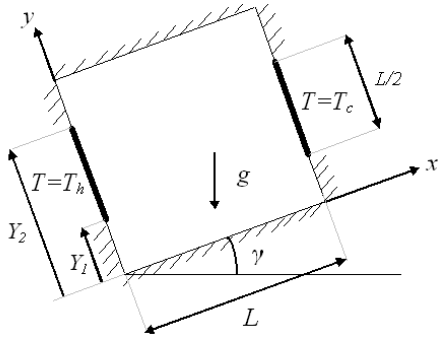

Figure 1. Geometry and coordinates of the cavity

3. NUMERICAL PROCEDURE

The governing equations and the associated boundary conditions are solved numerically using the finite volume method. The diffusion terms in the governing equations are discretized using the central difference scheme; while, an upwind scheme is employed for the convective terms. A staggered grid system together with the SIMPLER-algorithm is adopted to solve for the pressure and the velocity components. The solution of the fully coupled discretized equations is obtained iteratively using the TDMA method.

3.1. Grid Testing and Code Validation An extensive grid testing procedure was performed in order to guarantee mesh independent solutions. Four different uniform grids, namely, 15×15, 31×31, 61×61, and 121×121 were employed to simulate the natural convection inside a cavity with the heat source and heat sink positioned at the middle of the vertical walls for Ra=10^5 and φ=0.05. The vertical velocity profiles at the centerline of the cavity, i.e. $Y=L/2$, for these grids are shown in Figure 2. As the Figure shows, a 61×61 uniform grid is sufficiently fine to ensure a grid independent solution. Hence, this grid was used in all the subsequent calculations.

In order to validate the proposed numerical scheme, the buoyancy-driven heat transfer in a differentially-heated square cavity filled with air was analyzed using the code and the results were compared with the results of other investigators. The left wall of the cavity was kept hot; while, its right wall was cooled. Its top and bottom walls

were kept insulated. A 61×61 uniform grid was used for the calculations. Table 2 compares the average Nusselt number obtained by the present simulation with the results of other investigators for different Rayleigh numbers. It is observed from this Table, that good agreements exist between the results of the present code and the results of other investigators for the entire range of considered Rayleigh numbers. - Figure 3 shows a comparison between the results of the present code for the Nusselt number and the experimental results of Jahanshahi et al. [23] for different volume fractions of the nanoparticles. For the three considered Rayleigh numbers, $Ra=10^5$, 10^6 and 10^7 excellent agreements are observed between the two results for different volume fractions of the nanoparticles. Moreover, the variation of the average Nusselt number with respect to the volume fraction of the nanoparticles for $Ra=10^7$ obtained by the present simulation has a trend similar to that of the results of Jahanshahi et al.

4. RESULTS AND DISCUSSION

Having validated the code performance, the numerical scheme was then employed to study the natural convection in a rectangular cavity with partially active side walls filled with the nanofluids. Using the code, a parametric study was performed and the effects of the pertinent parameters, such as, the Rayleigh number, the position of the source and the sink, and the volume fraction of the nanoparticles on the fluid flow and heat transfer inside the cavity were investigated. Three different configurations of the source and the sink, namely, top-bottom, middle-middle, and bottom-top were considered in this study. All the results presented below are for the

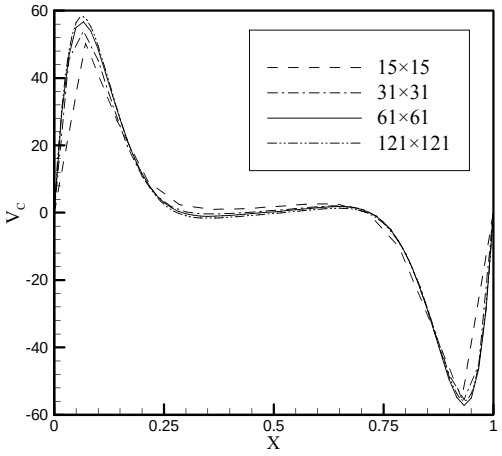

Figure 2. The effect of grid density on the vertical centerline velocity ($Y=L/2$) for the middle-middle case, $Ra=10^5$ and $\varphi=0.05$

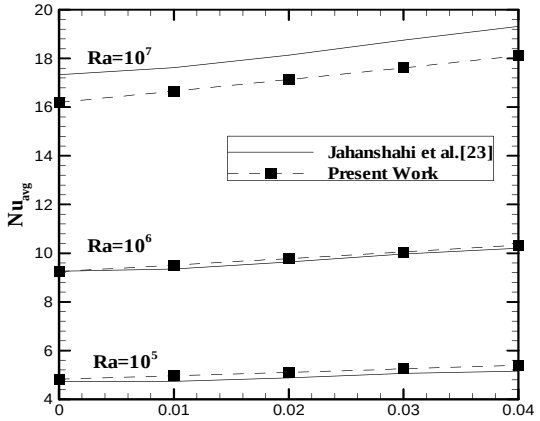

Figure 3. Variations of the average Nusselt number with respect to the volume fraction of nanoparticles for different Rayleigh numbers:
Comparison between the present work and results of [23]

TABLE 2. The average Nusselt number for various Rayleigh numbers: Comparisons between the present results and the results of other investigations

	$Ra=10^3$	$Ra=10^4$	$Ra=10^5$	$Ra=10^6$
Present work	1.139	2.291	4.603	8.857
Khanafer et al. [7]	1.118	2.245	4.522	8.826
Barakos and Mitsoulis [24]	1.114	2.245	4.510	8.806
Markatos and Pericleous [25]	1.108	2.201	4.430	8.754
De Vahl Davis [26]	1.118	2.243	4.519	8.799
Fusegi et al. [27]	1.105	2.302	4.646	9.012

Prandtl number of the base fluid equal to 5.83.

Figure 4 shows the streamlines and the isotherms for the Cu-water nanofluid (φ=0.15) with different positions of the source and the sink on the vertical walls at Ra=10^3. For the sake of comparisons, the streamlines and the isotherms for pure water (φ=0.0) are also shown in this Figure. For $Ra=10^3$, the heat transfer inside the cavity is mainly through conduction. A clockwise vortex is developed inside the cavity in this case. At this Rayleigh number, changing the locations of active portions of the side walls do not have a significant effect on the streamline patterns. However, as can be seen from Figure 4, changing the positions of the active portions of the side walls have a dramatic effect on the temperature distribution inside the cavity at Ra=10^3.

Figure 5 shows the streamlines and the isotherms for the Cu-water nanofluid (φ=0.15) with different positions of the source and the sink on the vertical walls at Ra=10^4. For the sake of comparisons, the streamlines and the isotherms for pure water (φ=0.0) are also shown in this Figure. With increasing the Rayleigh number, the effect of the convection becomes more significant and distinct boundary layers form along the active walls. The more packed streamlines and isotherms in the boundary layers along the active walls indicate higher velocities and intense convection in these areas. The core region of the cavity is relatively stagnant. The isotherms in the stratified core region are nearly parallel to the horizontal walls of the cavity.

The streamlines and the isotherms for the Cu-water nanofluid (φ=0.15) with different positions of the active portions of the side walls at Ra=10^5, are shown in Figure 6, respectively. The results for pure water (φ=0.0) are also shown in this Figure for the comparison purposes. Figure 6-a shows two distinct inner cells near the active walls in the top-bottom case. As can be seen from Figure 6-b, for the middle-middle case, a single cell with enlarged centre is formed inside the cavity. As Figure 6-c shows, for the bottom-top configuration, the flow has a single cell with a protracted centre. The core of the cell is straight for the base fluid, but it is inclined for the nanofluid. The maximum and the minimum values of the stream functions ($|\Psi|_{max} = 7.8$ and $|\Psi|_{min} = 3.4$) occur for the middle-middle and the top-bottom configurations, respectively. As can be seen from Figure 6, the temperature gradient is quite large in the vicinity of the active portions of the side walls. The heat transfer in these regions is mainly through convection. Moreover, in the stratified case region of the cavity, the isotherms are nearly horizontal and the heat transfer is conduction dominated. The isotherms are more condensed in this region for the middle-middle case (Figure 6-b).

The streamlines and the isotherms for the Cu-water nanofluid (φ=0.15) and different positions of the active portions of the side walls at Ra=10^6, are shown in Figure 7. The results for pure water (φ=0.0) are also shown in this Figure for the comparison purposes. As it is observed from these Figures, for this convection-dominated heat transfer, the streamlines, and the isotherms are more packed next to the active side walls. Moreover, the core region is protracted along the horizontal direction for all the cases considered in the Figures. In the bottom-top cases, a single protracted central cell is formed for the base fluid but two secondary inner cells are formed for the nanofluid. The secondary inner cells in the bottom-top case are of the same size. The isotherms are condensed in the cavity centre and near the active walls. The maximum and the minimum values of the stream functions ($|\Psi|_{max} = 12.1$ and $|\Psi|_{min} = 5.5$) occur for the middle-middle and the top-bottom cases, respectively.

Figures 8, 9 and 10 show the variation of the average Nusselt number with respect to the volume fraction of the nanoparticles at different Rayleigh numbers for three different configurations of the heat source and the heat sink, namely, the top-bottom, the middle-middle and the bottom-top cases, respectively. As these Figures show, the average Nusselt number varies linearly with the volume fraction of the nanoparticles. Moreover, the results show heat transfer enhancement as the Rayleigh number and/or the volume fraction of the nanoparticles increase. Moreover, as can be seen from these Figures, by increasing the Rayleigh number from 10^3 to 10^6, the average Nusselt number of the base fluid is increased by about 195 percent for the top-

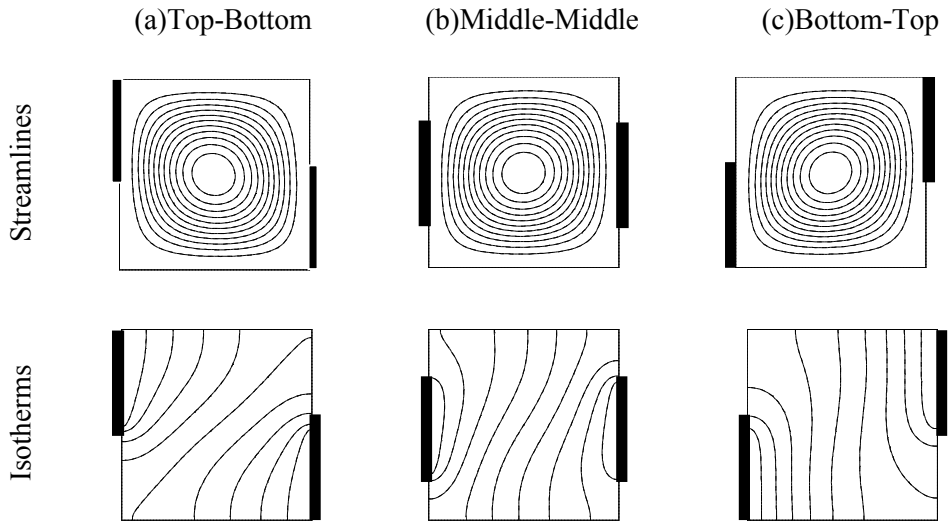

Figure 4. Streamlines and isotherms for different positions of the source and the sink at $Ra=10^3$, — for $\varphi=0.0$, --- for $\varphi=0.15$

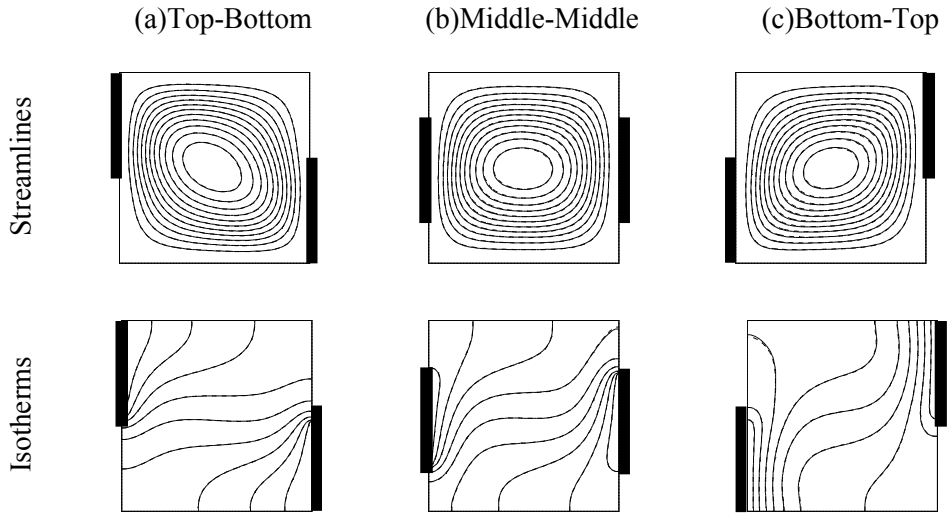

Figure 5. Streamlines and isotherms for different positions of the source and the sink at $Ra=10^4$, — for $\varphi=0.0$, --- for $\varphi=0.15$

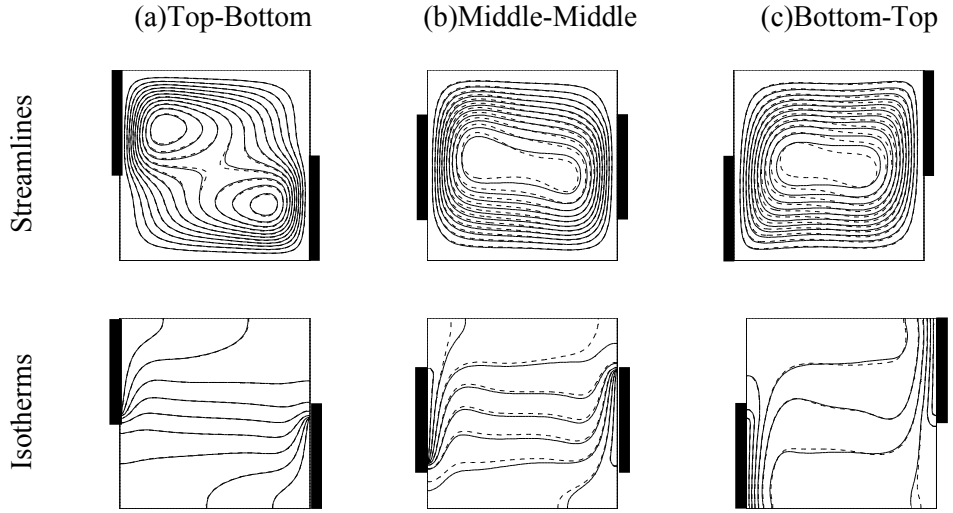

Figure 6. Streamlines and isotherms for different positions of the source and the sink at $Ra=10^5$, — for $\varphi=0.0$, --- for $\varphi=0.15$

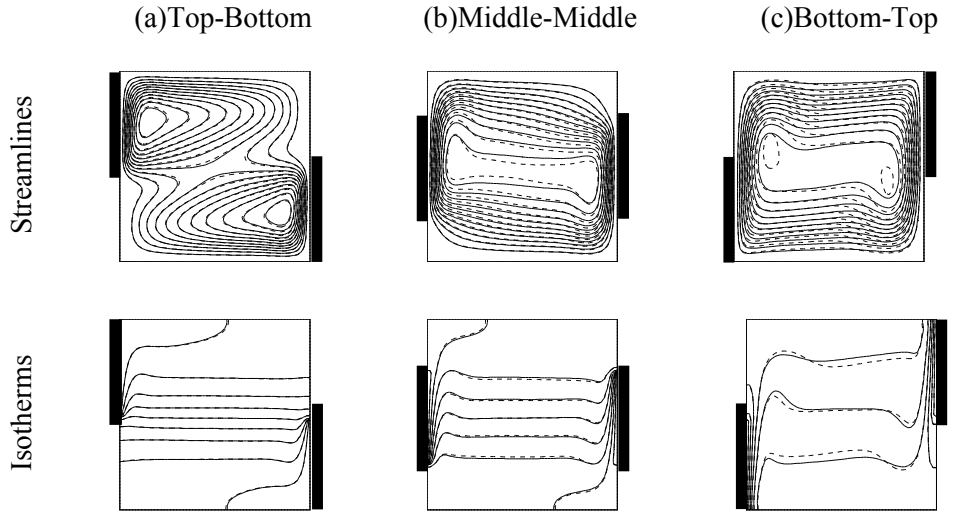

Figure 7. Streamlines and isotherms for different positions of the source and the sink at $Ra=10^6$, — for $\varphi=0.0$, --- for $\varphi=0.15$

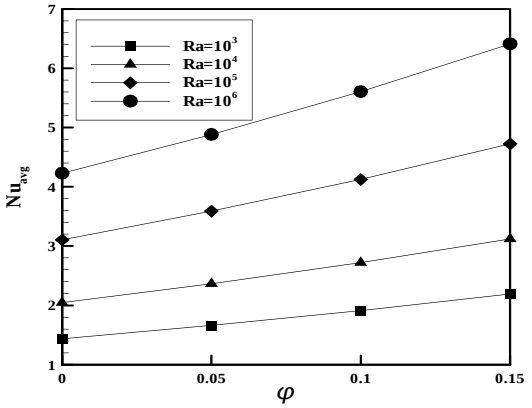

Figure 8. Variations of the average Nusselt number for the top-bottom location of the active parts with respect to the volume fraction of nanoparticles at different Rayleigh numbers

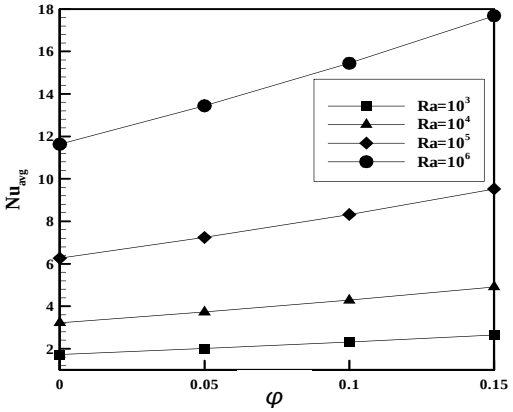

Figure 9. Variations of the average Nusselt number for the middle-middle location of the active parts with respect to the volume fraction of nanoparticles at different Rayleigh numbers

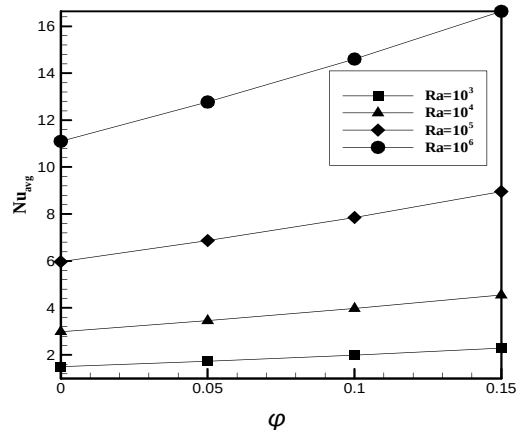

Figure 10. Variations of the average Nusselt number for the bottom-top location of the active parts with respect to the volume fraction of nanoparticles at different Rayleigh numbers

bottom case and by about 517 percent for the middle-middle case, as well as, by about 410 percent for the bottom-top case; while, the average Nusselt number for the nanofluid with φ=0.15 is increased by about 193 percent for the top-bottom case and by about 512 percent for the middle-middle case, as well as, by about 400 percent for the bottom-top case. Increasing the volume fraction of the nanoparticles from 0.0 to 0.15 causes almost 53 percent increase in the average Nusselt number for both the top-bottom, and middle-middle locations of the active parts, and about 50 percent increase in average Nusselt number for bottom-top active parts location at $Ra=10^6$.

The streamlines and the isotherms for the Cu-water nanofluid (φ=0.1) for the case of middle-middle active side walls with different inclination angles at $Ra=10^6$ are shown in Figures 11 and 12, respectively. For the sake of comparisons, the streamlines and the isotherms for pure water (φ=0.0) are also shown in these Figures. As can be seen from Figure 11, by increasing the inclination angle from 0 to 90°, the protracted core changes into a circle. As observed from Figure 12, by increasing the inclination angle from 0 to 90°, the straight isotherms in middle of the cavity change into curve ones with two small cores. Figures 13 and 14 show the variation of the average Nusselt number with respect to the inclination angle at different Rayleigh numbers for pure fluid (φ=0.0) and Cu-water nanofluid (φ=0.1) in the considered middle- middle case, respectively. As this Figure shows, for nearly all of the Rayleigh numbers, with increasing the inclination angle from 0 to 30°, the average Nusselt number increases. However, for these Rayleigh numbers, the Nusselt number decreases by increasing the inclination angle from 30° to 90°. For $Ra=10^4$ the average Nusselt number increases by increasing the inclination angle from 0° to 45°, and decrease by increasing the angle further from 45° to 90°.

5. CONCLUSIONS

The buoyancy-driven fluid flow and heat transfer in a square cavity with partially active side walls filled with Cu-water nanofluid have been simulated using the finite volume method. A parametric study was undertaken and the effects of the position of active portions of the side walls,

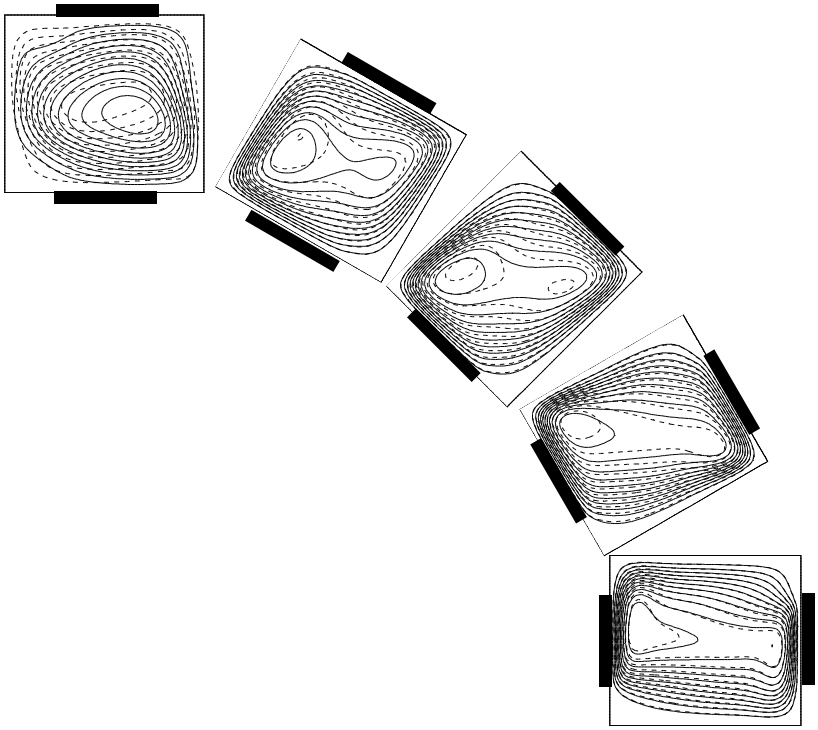

Figure 11. Streamlines for different inclination angles of the cavity (from 0 to 90°) in middle- middle case at $Ra=10^6$, — for φ=0.0, --- for φ=0.1

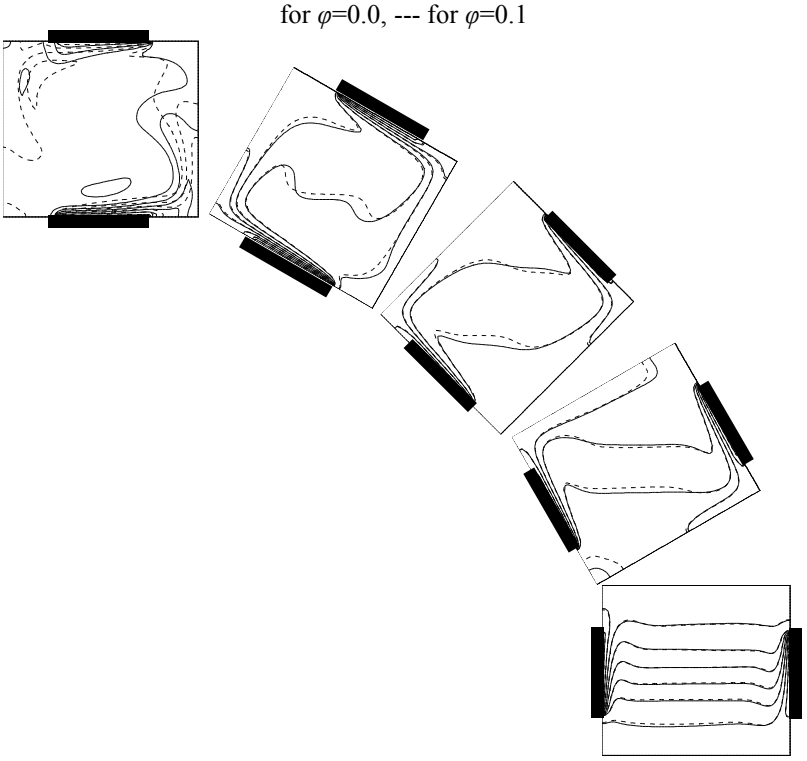

Figure 12. Isotherms for different inclination angles of the cavity (from 0 to 90°) in middle- middle case at $Ra=10^6$, — for φ=0.0, --- for φ=0.1

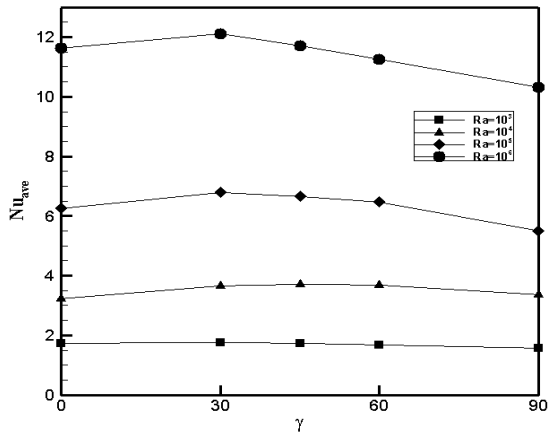

Figure 13. Variations of the average Nusselt number for the middle-middle location of the active parts with respect to the inclination angle of cavity at different Rayleigh numbers for φ=0.0

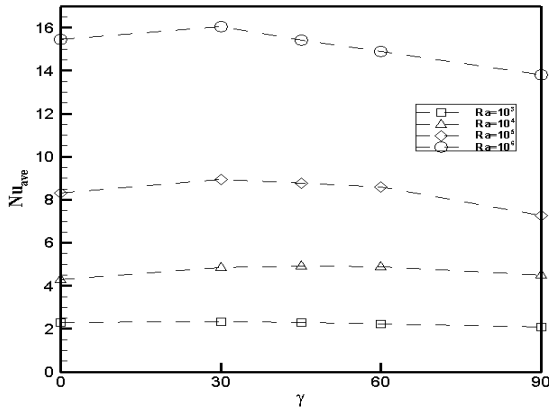

Figure 14. Variations of the average Nusselt number for the middle-middle location of the active parts with respect to the inclination angle of cavity at different Rayleigh numbers for φ=0.1

and the volume fraction of the nanoparticles on the heat transfer inside the cavity were investigated. The results show that, for all the considered Rayleigh numbers, the maximum and the minimum average Nusselt number occurred for the middle-middle and the top-bottom cases of the active portions of the side walls, respectively. Moreover, the heat transfer rate increased with increasing the volume fraction of the nanoparticles. With exception to $Ra=10^4$, heat transfer rate increases with increasing the inclination angle from 0 to 30˚ and decreases from 30˚ to 90˚.

6. REFERENCE

1. Choi, U.S., "Enhancing thermal conductivity of fluids with nanoparticles", ***ASME, FED***, Vol. 231, No. 66, (1995), 99–105.
2. Das, S.K., Choi, S.U.S., Yu, W. and Pradeep, T., "Nanofluids: science and technology", John Wiley & Sons Inc, New York, (2007), 1-38.
3. Xuan, Y. and Li, Q., "Heat transfer enhancement of nanofluids", ***International Journal of Heat and Fluid Flow***, Vol. 21, No. 1, (2000), pp. 58–64.
4. Xie, H.Q., Wang, J.C., Xi, T.G., Li, Y. and Ai, F., "Dependence of the thermal conductivity of nanoparticle–fluid mixture on the base fluid", ***Journal of Materials Science Letters***, Vol. 21, No. 19, (2002), 1469–1471.
5. Heyhat, M.M. and Kowsary, F., "Numerical simulation of forced convection of nanofluids by a two-component nonhomogeneous model", ***International Journal of Engineering***, Vol. 23, No. 1, (2010), 89-99.
6. Shokouhmand, H. and Sayehvand, H., "Numerical study of flow and heat transfer in a square driven cavity", ***International Journal of Engineering***, Vol. 17, No. 3, (2004), 301-317.
7. Khanafer, K., Vafai, K. and Lightstone, M., "Buoyancy-driven heat transfer enhancement in a two-dimensional enclosure utilizing nanofluids", ***International Journal of Heat and Mass Transfer***, Vol. 46, No. 19, (2003), 3639–3653.
8. Maiga, S.E.B., Palm, S.J., Nguyen, C.T., Roy, G. and Galanis, N., "Heat transfer enhancement by using nanofluids in forced convection flows", ***International Journal of Heat and Fluid Flow***, Vol. 26, No. 4 (2005), 530–546.
9. Jou, R.Y. and Tzeng, S.C., "Numerical research of nature convective heat transfer enhancement filled with nanofluids in rectangular enclosures". ***International Communications in Heat and Mass Transfer***, Vol. 33, No. 6, (2006), 727–736.
10. Polidori, G., Fohanno, S. and Nguyen, C.T., "A note on heat transfer modeling of Newtonian nanofluids in laminar free convection", ***International Journal of Thermal Sciences***, Vol. 46, No. 8, (2007), 739–744.
11. Valencia, A. and Frederick, R.L., "Heat transfer in square cavities with partially active vertical walls", ***International Journal of Heat and Mass Transfer***, Vol. 32, No. 8, (1989), 1567–1574.
12. Deng, Q.H., Tang, G.F. and Li, Y.,"A combined temperature scale for analyzing natural convection in rectangular enclosures with discrete wall heat sources", ***International Journal of Heat and Mass Transfer***, Vol. 45, No. 16, (2002), 3437–3446.
13. Nithyadevi, N., Kandaswamy, P. and Lee, J., 2007. "Natural convection in a rectangular cavity with partially active side walls", ***International Journal of Heat and Mass Transfer***, Vol. 50 , No. 23-24, (2007), 4688–4697.
14. Sheikhzadeh, G.A., Babaei, M.R., Rahmany, V. and Mehrabian, M.A., "The effects of an imposed magnetic

field on natural convection in a tilted cavity with partially active vertical walls: Numerical approach", ***International Journal of Engineering***, Vol. 23, No. 1, (2010), 65-78.

15.] Oztop, H.F. and Abu-Nada, E., "Numerical study of natural convection in partially heated rectangular enclosures filled with nanofluids", ***International Journal of Heat and Fluid Flow***, Vol. 29, No. 5, (2008), 1326–1336.

16. Polentini, M.S., Ramadhyani, S. and Incropera, F.P., "Single-phase thermosyphon cooling of an array of discrete heat sources in a rectangular cavità", ***International Journal of Heat and Mass Transfer***, Vol. 36, No. 16, (1993), 3983-3996.

17. Kenjereš, S., Gunarjo, S.B., and Hanjalić, K., "Natural convection in an air- filled cubical cavity under different angles of inclinations", Proceeding of the ICHMT second Int. Symp, NewYork, (2001), 1357-1364.

18. Cianfrini, C., Corcione, M. and Dell'Omo, P.P., "Natural convection in titled square cavities with differentially heated opposite walls", ***International Journal of Thermal Sciences***, Vol. 44, No. 5, (2005), 441-451.

19. Baïri, A., "Nusselt–Rayleigh correlations for design of industrial elements: Experimental and numerical investigation of natural convection in tilted square air filled enclosures***", Energy Conversion and Management***, Vol. 49, No. 4, (2008), 771-782.

20. Baïri, A., García de María, J.M., Laraqi, N. and Alilat, N., "Free convection generated in an enclosure by alternate heated bands. Experimental and numerical study adapted to electronics thermal control", ***International Journal of Heat and Fluid Flow***, Vol. 29, No. 5, (2008), 1337-1346.

21. Corcione, M. and Habib, E., "Buoyant heat transport in fluids across tilted square cavities discretely heated at one side", ***International Journal of Thermal Sciences***, Vol. 49, No. 5, (2010), 797-808.

22. Brinkman, H.C., "The viscosity of concentrated suspensions and solutions", ***The Journal of Chemical Physics***, Vol. 20, No. 4 , (1952), 571–581.

23. Jahanshahi, M., Hosseinizadeh, S.F., Alipanah, M., Dehghani, A., and Vakilinejad, G.R., "Numerical simulation of free convection based on experimental measured conductivity in a square cavity using Water/SiO2 nanofluid", ***International Communications in Heat and Mass Transfer***, Vol. 37, No. 1, (2010), 687-694.

24. Barakos, G. and Mitsoulis, E., "Natural convection flow in a square cavity revisited: laminar and turbulent models with wall functions", ***International Journal for Numerical Methods in Fluids***, Vol. 18, No. 7 , (1994), 695–719.

25. Markatos, N.C. and Pericleous, K.A., "Laminar and turbulent natural convection in an enclosed cavity", ***International Journal of Heat and Mass Transfer***, Vol. 27, No. 5, (1984), 772–775.

26. De Vahl Davis, G., "Natural convection of air in a square cavity, a benchmark numerical solution", ***International Journal for Numerical Methods in Fluids,*** Vol. 3, No. 3 , (1983), 249–264.

27. Fusegi, T., Hyun, J.M., Kuwahara, K. and Farouk, B., "A numerical study of three dimensional natural convection in a differentially heated cubical enclosure", ***International Journal of Heat and Mass Transfer***, Vol. 34, No. 6, (1991), 1543–1557.